Figures and figure supplements

Serine ADP-ribosylation marks nucleosomes for ALC1-dependent chromatin remodeling

Jugal Mohapatra *et al*

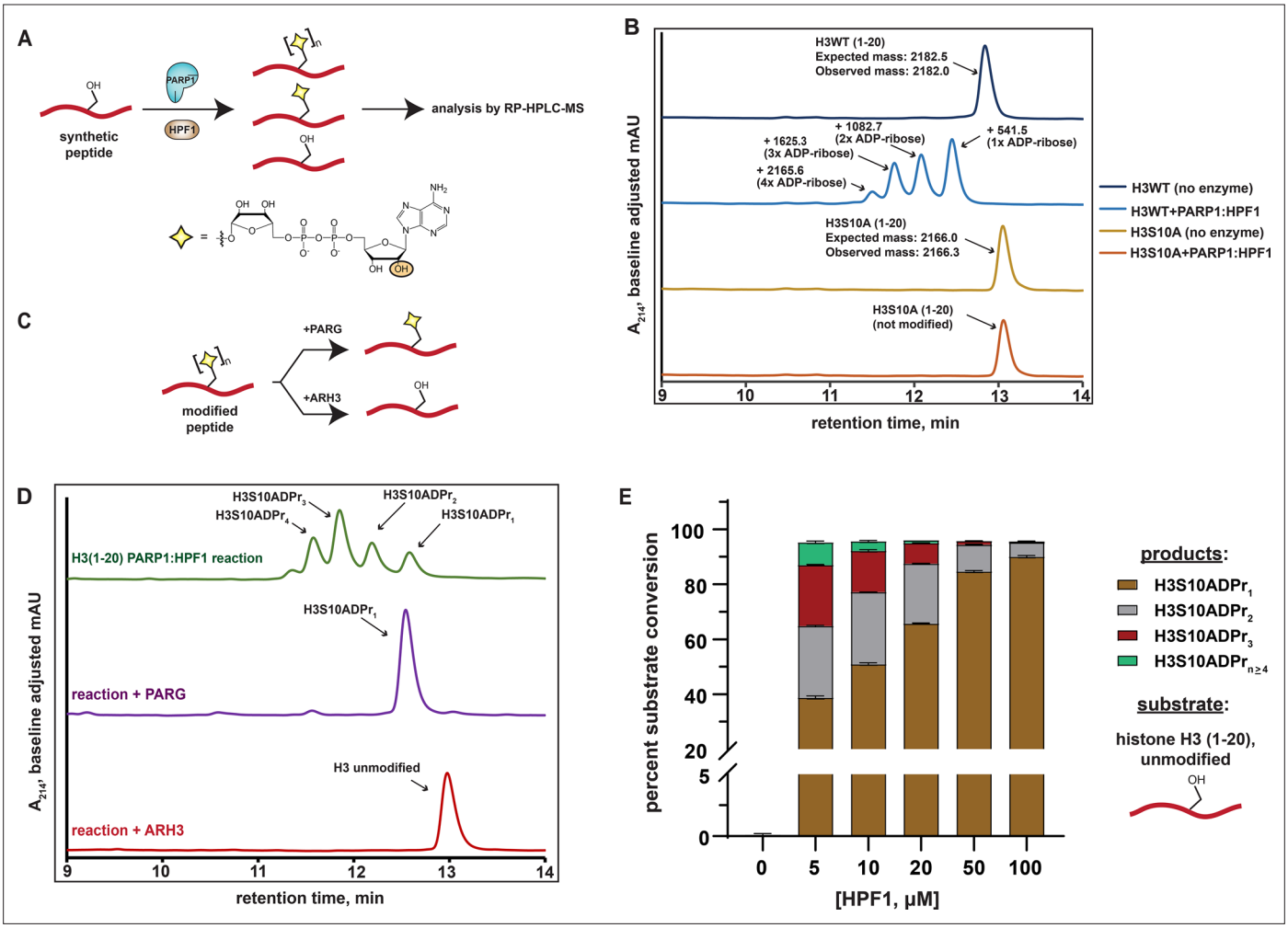

Figure 1. Analysis of serine mono- and poly-ADPr by the PARP1:HPF1 complex on synthetic peptide substrates. (**A**) A schematic showing the workflow employed to analyze peptide poly-APDr by the recombinant PARP1:HPF1 complex. Peptide products are separated by polymer length via RP-HPLC. The yellow star represents a serine-linked ADP-ribose modification, 'n' represents variable polymer length, and the orange circle indicates the site of linear ADP-ribose polymerization. (**B**) RP-HPLC and MS analysis of substrate peptides (histone H3 wild-type or S10A mutant, amino acids 1–20) and corresponding PARP1:HPF1 reaction products (for raw MS data, see ***Supplementary file 1***). RP-HPLC gradients are from 0 to 35% Solvent B (2–22 min). (**C**) A schematic describing the ADP-ribosylhydrolase-based characterization strategy. Enzymes and their respective reaction products are depicted. (**D**) RP-HPLC traces from PARG- or ARH3-treated H3 peptide ADPr reactions that were optimized for ADP-ribose chain elongation. The number of ADP-ribose units was verified by MS analysis. (**E**) Product analysis of a PARP1 ADPr reaction in the presence of increasing HPF1 concentrations. Histone H3 substrate peptide starting material and each unique ADP-ribosylated product were quantified via HPLC chromatogram peak integration (see Methods and ***Figure 1—figure supplement 1D***). The columns represent the percent substrate conversion to each ADP-ribosylated product. Data are represented as mean ± s.d. (n = 3).

A

ANALYTE	MRM TRANSITION (Parent/daughter, Da)	INTEGRATED PEAK AREA
Adenosine	268.0/136.0	2160000
Ribosyl-adenosine	400.0/136.0	45800000
Diribosyl-adenosine	532.2/136.0	7870

$$\text{Branching frequency} = \frac{\text{(peak area of diribosyl-adenosine)}}{\text{(peak area of ribosyl-adenosine)}} = 1.7 \times 10^{-4} \text{ OR } 0.017\%$$

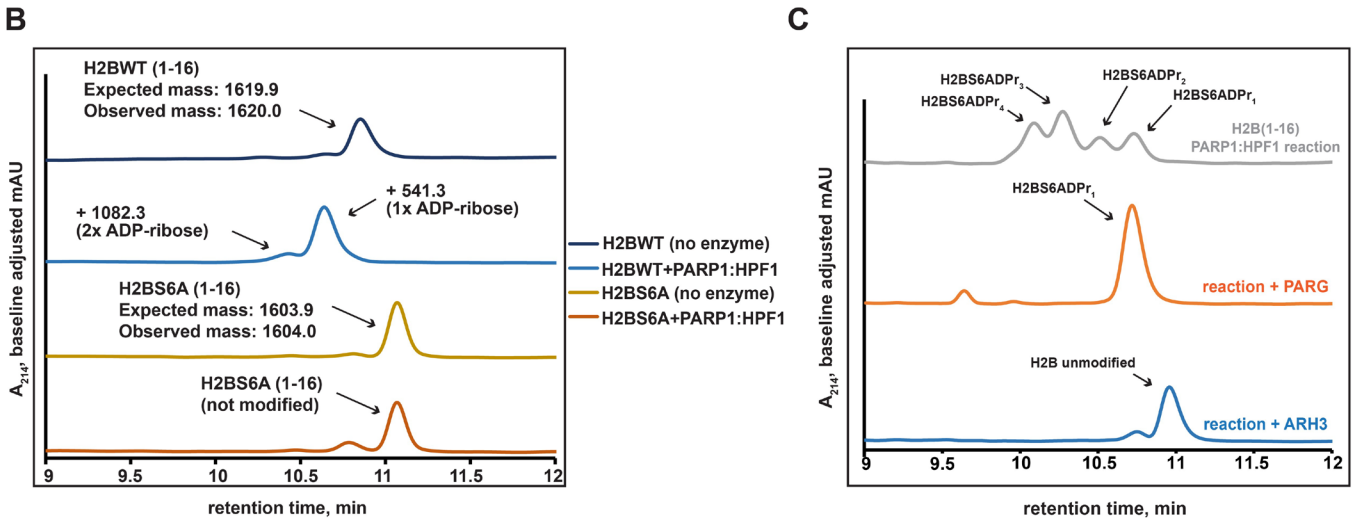

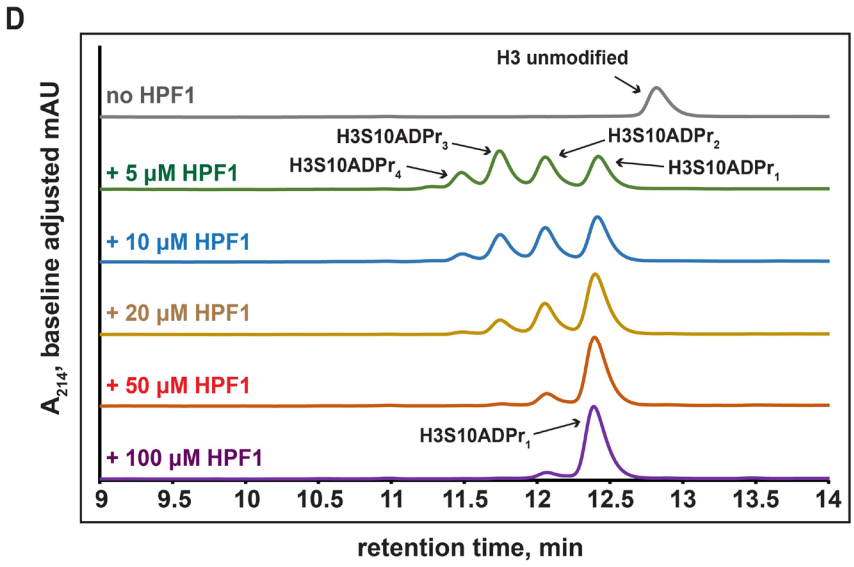

Figure 1—figure supplement 1. The recombinant PARP1:HPF1 complex installs linear poly-ADP-ribose chains at biologically relevant target sites. (**A**) Summary of LC-MS/MS analysis of enzymatic digestion products from PAR chains installed on a peptide using our technology. The spectra were produced on a Sciex QTRAP 6500+ mass spectrometer. (**B**) RP-HPLC and MS analysis of substrate peptides (H2B wild-type or S6A mutant, amino acids 1–16) and corresponding PARP1:HPF1 reaction products. RP-HPLC gradients are from 0 to 35% Solvent B (2–22 min). (**C**) RP-HPLC traces from PARG- or

Figure 1—figure supplement 1 continued on next page

Figure 1—figure supplement 1 continued

ARH3-treated H2B peptide ADPr reactions that were optimized for ADP-ribose chain elongation. The number of ADP-ribose units was verified by MS analysis. (**D**) Representative RP-HPLC analyses of ADPr reactions from ***Figure 1E*** containing PARP1 (1 μM), unmodified H3 substrate peptide (amino acids 1–20; 180 μM), NAD^+ (2 mM), and various HPF1 concentrations (indicated on corresponding trace). RP-HPLC gradients are from 0 to 35% Solvent B (2–22 min). For peak area integration values, see Supplementary Dataset.

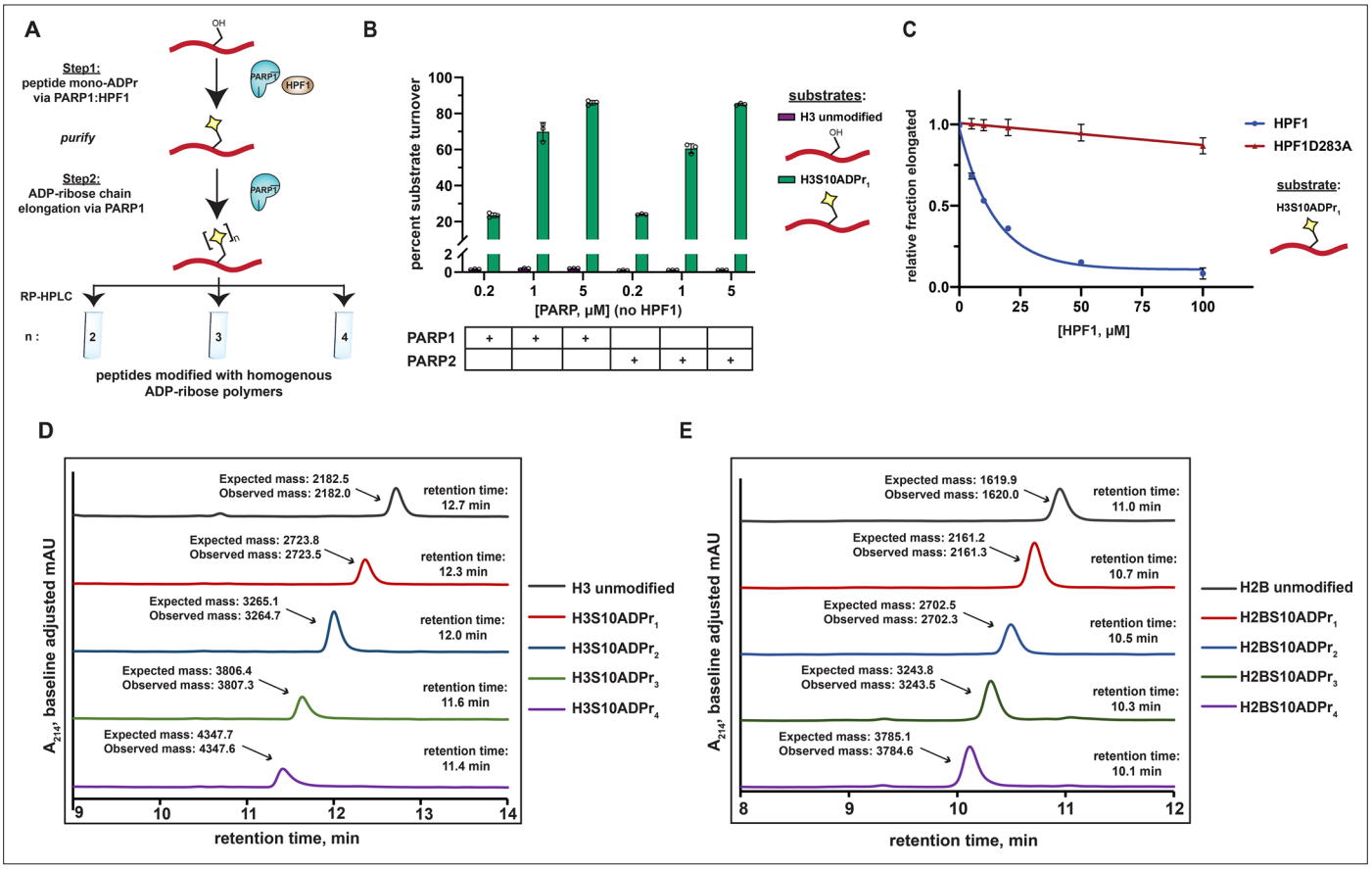

Figure 2. A two-step enzymatic process to prepare poly-ADP-ribosylated peptides with defined ADP-ribose chain lengths. (**A**) A schematic showing the two-step enzymatic procedure implemented to synthesize and purify poly-ADP-ribosylated peptides. The mono-ADP-ribosylated peptide product from Step 1 was purified using preparative RP-HPLC prior to use in Step 2. (**B**) Substrate turnover analysis of PARP1 and PARP2 ADPr reactions in the absence of HPF1. Purple bars represent total percent turnover of an unmodified H3 peptide to mono- or poly-ADP-ribosylated products. Green bars represent total percent turnover of the H3S10ADPr$_1$ peptide to poly-ADP-ribosylated products (for poly-ADP-ribosylated product distribution, see ***Figure 2—figure supplement 1A*** and B). Data are represented as mean ± s.d. (n = 3). (**C**) Analysis of PARP1 elongation activity on the H3S10ADPr$_1$ peptide substrate in the presence of increasing amounts of HPF1 or HPF1D283A. Fraction elongated represents the fraction of H3S10ADPr$_1$ peptide converted to poly-ADP-ribosylated products. Data are normalized to fraction of substrate elongated in the absence of HPF1. Data are represented as mean ± s.d. (n = 3). The curves represent the fit of the data into a non-linear regression model for one-phase exponential decay. (**D**) RP-HPLC and MS analysis of mono- and poly-ADP-ribosylated H3 peptides that have been purified to homogeneity via semi-preparative HPLC. (**E**) As in (**D**), but for H2B (amino acids 1–16) peptides.

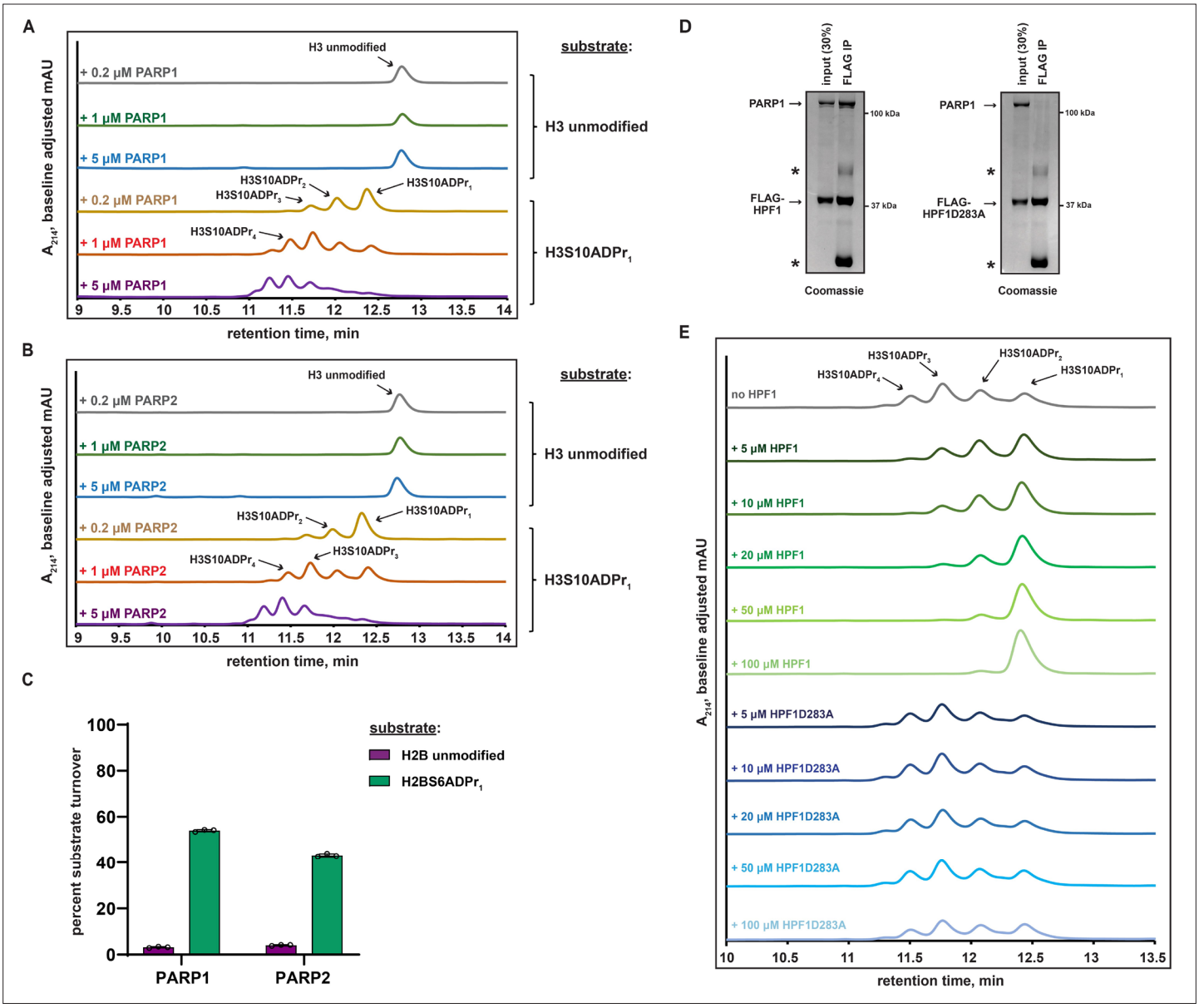

Figure 2—figure supplement 1. PARP1 and PARP2 efficiently elongate ADP-ribose chains from mono-ADP-ribosylated peptides. (**A**) Representative RP-HPLC analyses of ADPr reactions from ***Figure 2B*** containing various PARP1 concentrations (indicated on corresponding trace), unmodified H3 or H3S10ADPr$_1$ substrate peptide (amino acids 1–20; 180 μM), NAD$^+$ (2 mM), and no HPF1. RP-HPLC gradients are from 0 to 35% Solvent B (2–22 min). For peak area integration values, see Supplementary Dataset. (**B**) As in (**A**), but with various PARP2 concentrations (indicated on corresponding trace). (**C**) Substrate turnover analysis of ADPr reactions containing PARP1 (1 μM) or PARP2 (1 μM), the indicated H2B substrate peptide (amino acids 1–16; 40 μM), NAD$^+$ (2 mM), and no HPF1. Purple bars represent total percent turnover of an unmodified H2B peptide to mono- or poly-ADP-ribosylated products. Green bars represent total percent turnover of the H2BS6ADPr$_1$ peptide to poly-ADP-ribosylated products. For peak area integration values, see Supplementary Dataset. Data are represented as mean ± s.d. (n = 3). (**D**) Coomassie blue-stained SDS-PAGE gel showing FLAG-HPF1:PARP1 or FLAG-HPF1D283A:PARP1 immunoprecipitation (IP) experiments. *Gel migration species corresponding to the immunoglobulin chains from the anti-FLAG M2 magnetic beads. (**E**), Representative RP-HPLC analyses of ADPr reactions from ***Figure 2c*** containing PARP1 (1 μM), H3S10ADPr$_1$ substrate peptide (amino acids 1–20; 180 μM), NAD$^+$ (2 mM), and various HPF1 or HPF1D283A concentrations (concentration indicated on corresponding trace). RP-HPLC gradients are from 0 to 35% Solvent B (2–22 min). For peak area integration values, see Supplementary Dataset.

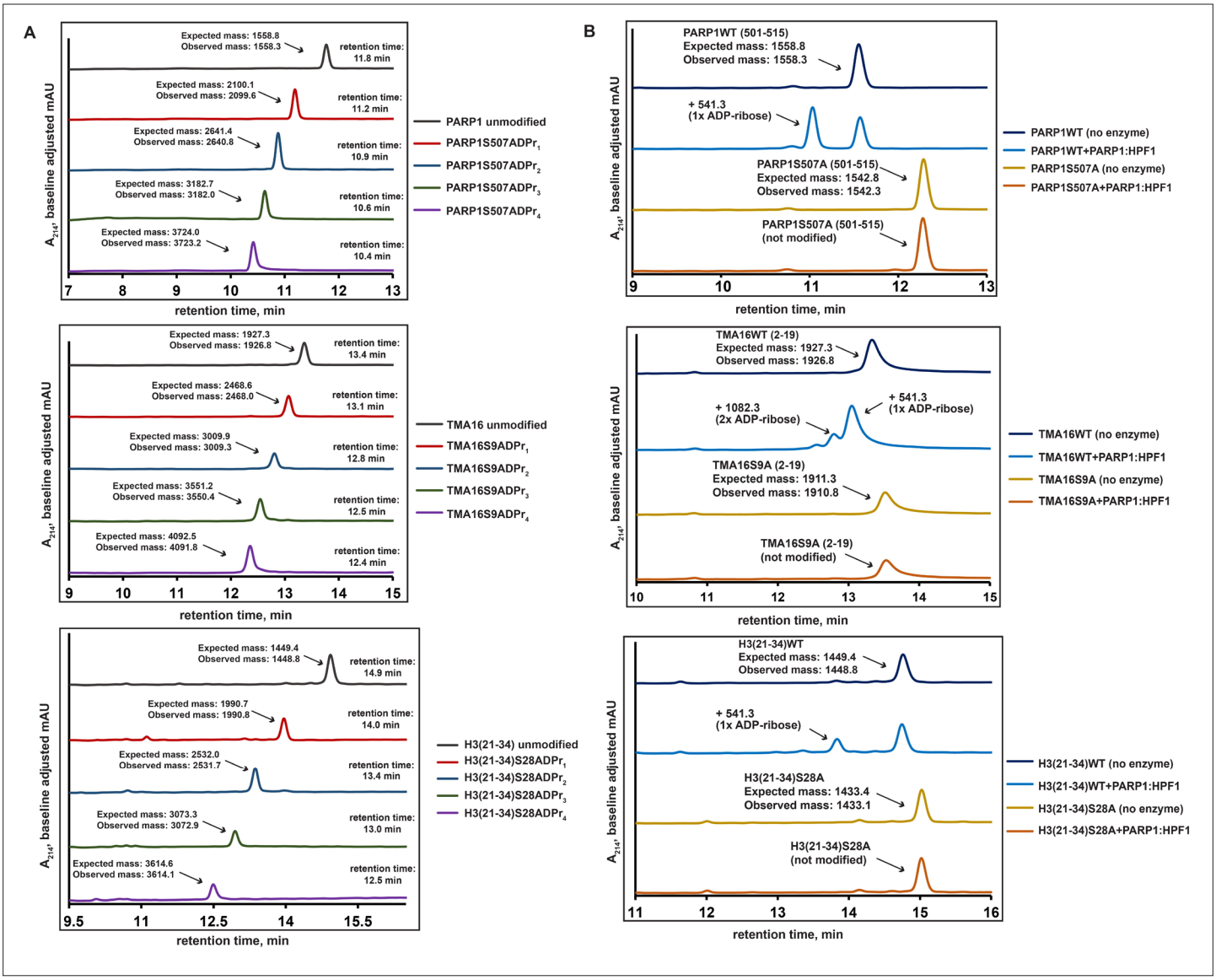

Figure 2—figure supplement 2. The two-step enzymatic process is broadly applicable to install poly-ADP-ribosylation at PARP1:HPF1 target sites. (**A**) RP-HPLC and MS analysis of mono- and poly-ADP-ribosylated PARP1(501-515), TMA16(2-19) and H3(21–34) peptides that have been purified to homogeneity using semi-preparative HPLC. RP-HPLC gradients are from 0 to 35% Solvent B (2–22 min) (**B**) RP-HPLC and MS analysis of substrate peptides (PARP1 wild-type or S507A mutant, TMA16 wild-type or S9A mutant, H3(21–34) wild-type or S28A mutant) and corresponding PARP1:HPF1 reaction products. RP-HPLC gradients are from 0 to 35% Solvent B (2–22 min). For LC-MS characterization, see ***Supplementary file 1***.

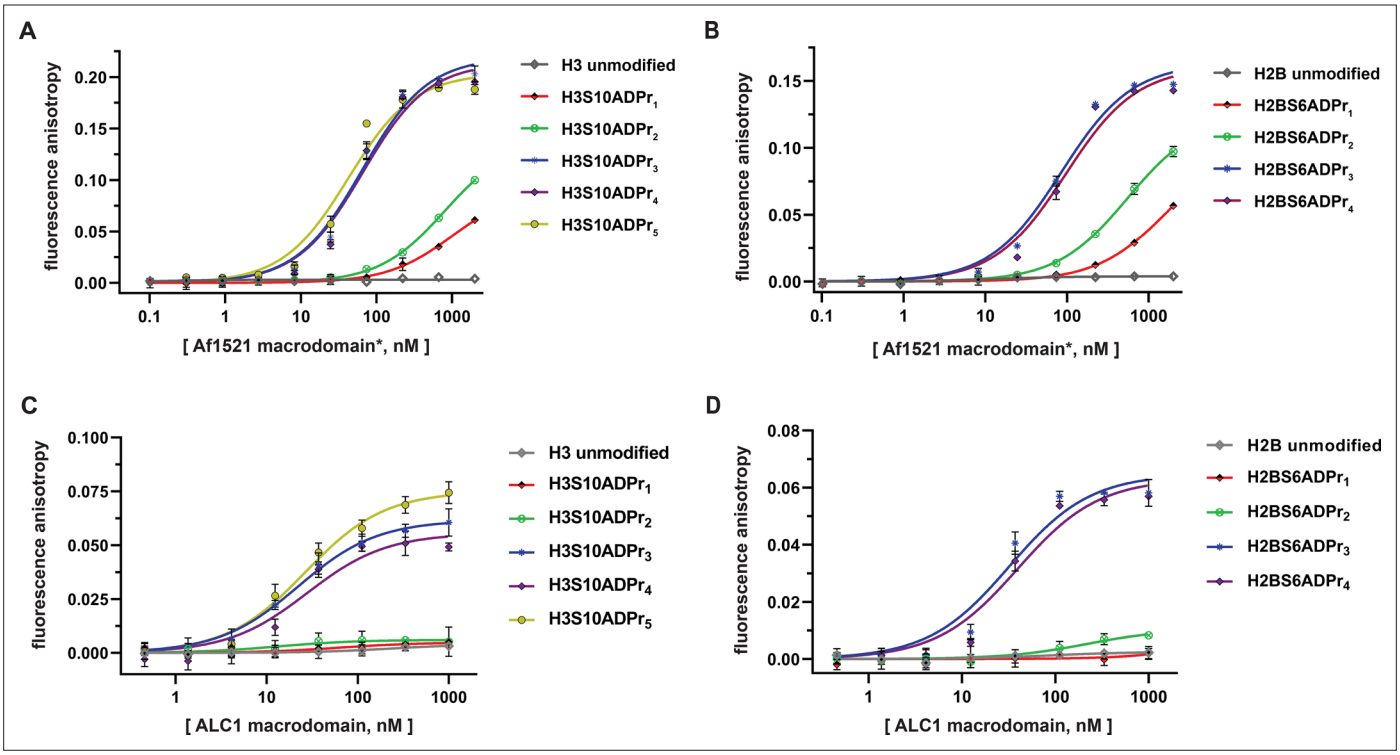

Figure 3. The ALC1 macrodomain engages ADP-ribosylated H2B and H3 peptides with equal affinity. (**A**) Fluorescence polarization (FP) assays to evaluate binding affinities of different ADP-ribosylated, fluorescein-labeled H3 (1–20) peptides to the Af1521 macrodomain. Data are represented as mean ± s.d. (n = 3). All curves represent fit of the data into a non-linear regression equation for one-site, specific binding (for $K_{d,\,app}$ values, see ***Supplementary file 4***). *The Af1521 macrodomain is from the commercially available pan-ADP-ribose detection reagent. (**B**) As in (**A**), but with fluorescein-labeled H2B (1-16) peptides. (**C**) FP assays as described in (**A**) to evaluate binding affinities of ADP-ribosylated, fluorescein-labeled H3 (1–20) peptides to the ALC1 macrodomain. (**D**) As in (**C**), but with fluorescein-labeled H2B (1-16) peptides.

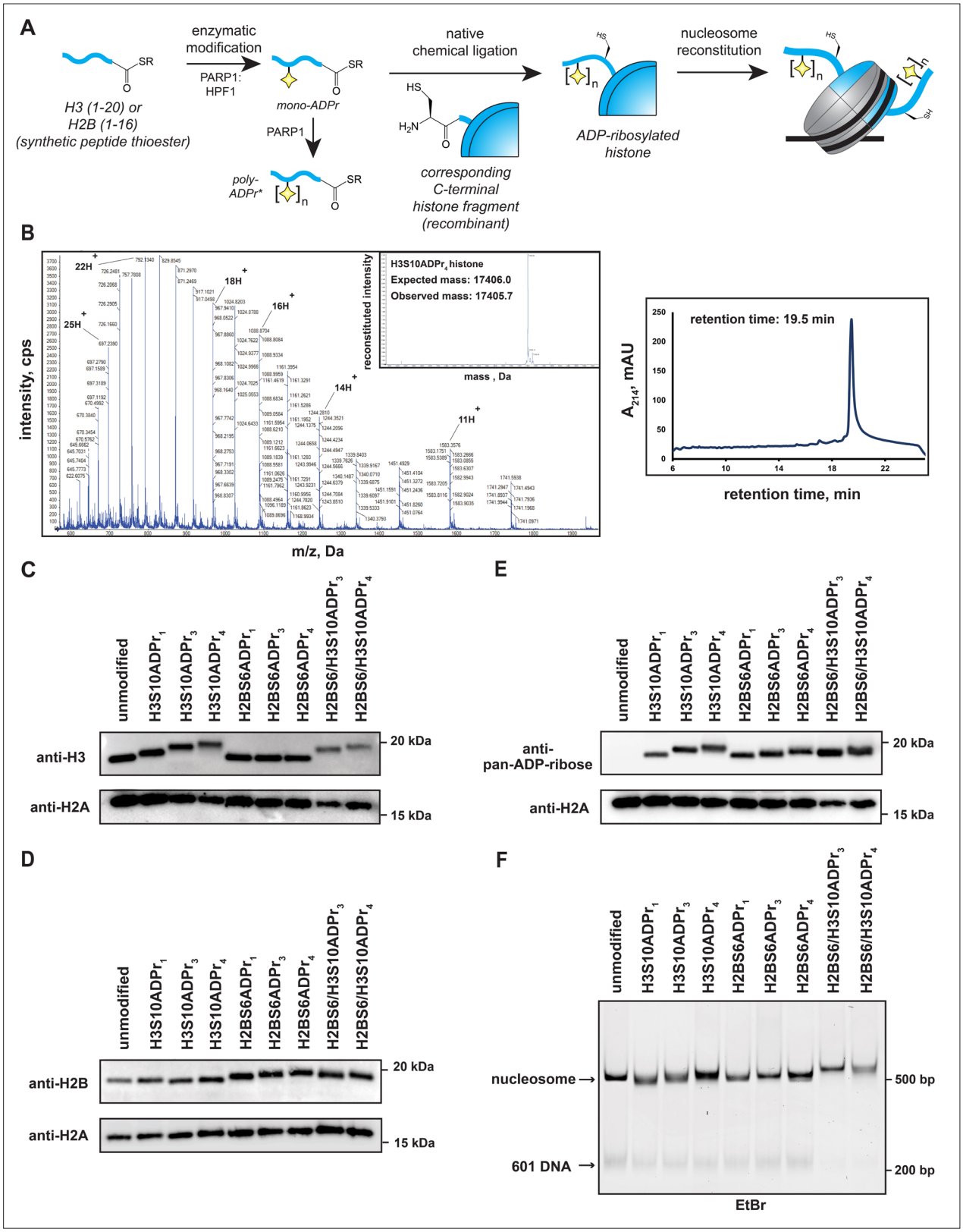

Figure 4. Installation of homogenous ADP-ribose polymers onto reconstituted nucleosomes via a chemoenzymatic strategy. (**A**) A schematic depicting the protein semi-synthesis-based strategy to install homogenous ADP-ribose polymers at specific sites on histone proteins. The nucleosome cartoon includes DNA (black line), as well as the histone protein octamer core (gray = recombinant histones, blue = semi-synthetic histone). *The poly-ADP-ribosylated peptides are separated via HPLC to yield homogenous species prior to the ligation reaction. (**B**) Representative HPLC/MS characterization

Figure 4 continued on next page

Figure 4 continued

of the full-length H3S10ADP$_4$ protein. Raw ESI-MS spectra, MS deconvolution, and RP-HPLC chromatogram are shown. RP-HPLC gradient is from 0 to 80% Solvent B (2–22 min). For additional histone HPLC and MS characterizations, see ***Supplementary file 5***. (**C**) Western blot analysis of histone H3 following nucleosome assembly. ADP-ribose-dependent gel migration shifts (12% bis-tris SDS-PAGE gel in MES running buffer) demonstrate sample homogeneity. (**D**) Histone H2B analysis as described in (**C**). (**E**) Pan-ADP-ribose western blot analysis of all assembled nucleosomes. (**F**) Native gel analysis of assembled nucleosomes. Single nucleosome bands and trace levels of free 601 DNA demonstrate sample homogeneity and assembly efficiency. EtBr = ethidium bromide stain.

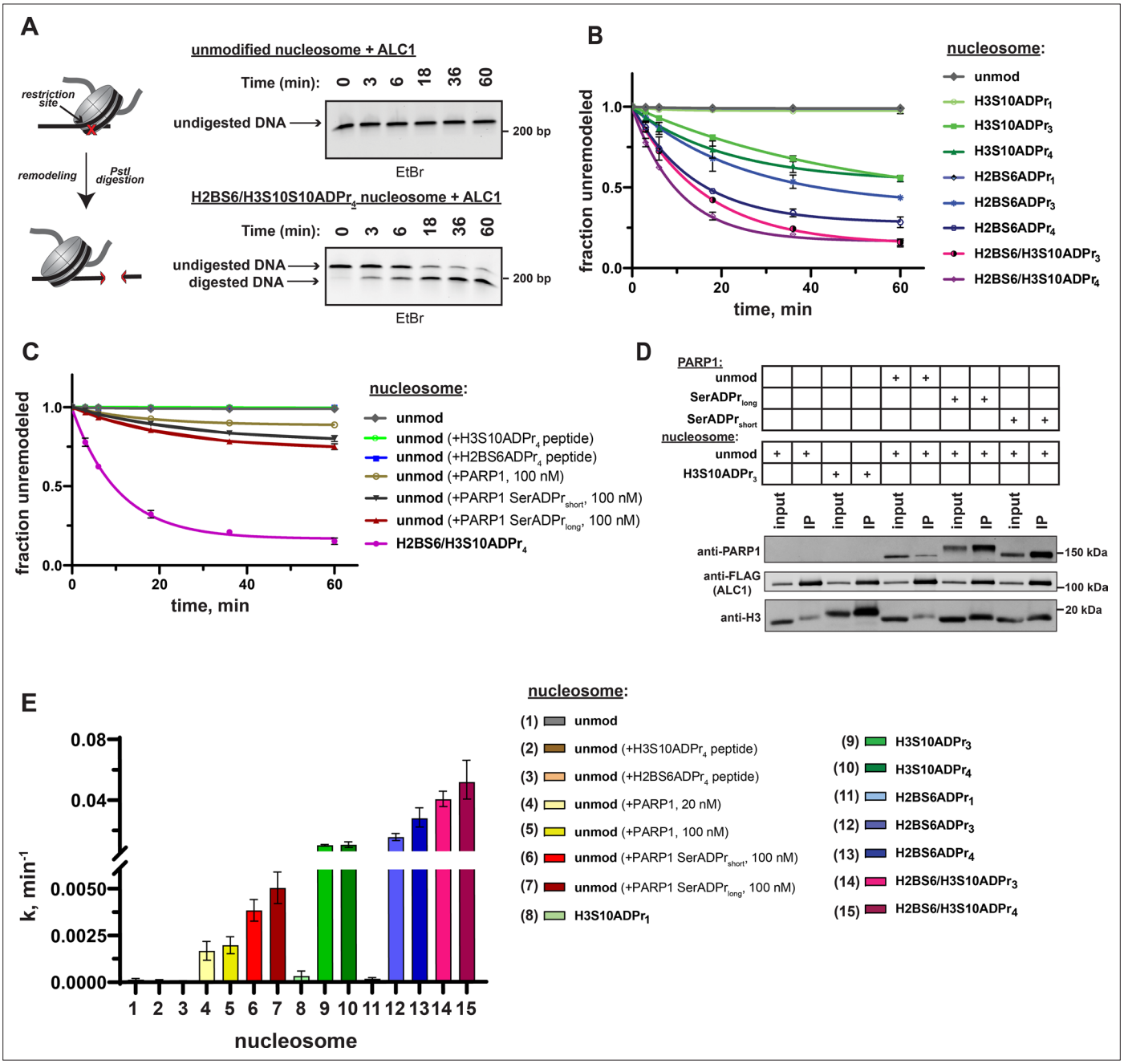

Figure 5. ADPr at H2BS6 and H3S10 convert nucleosomes into robust ALC1 substrates. (**A**) Schematic depicting the REA assay for chromatin remodeling and representative TBE gel analyses of recombinant ALC1 activity on unmodified or H2BS6/H3S10ADPr$_4$ nucleosomes. (**B**) ALC1 nucleosome remodeling assay time-course wherein each reaction comprises ALC1 and the indicated nucleosome ('unmod' = unmodified). (**C**) As in (**B**), but each reaction comprises ALC1, unmodified nucleosome (20 nM), and the indicated modified histone peptide or PARP1. Modified histone peptide concentration is equal to the corresponding full-length histone concentration (40 nM). The H2BS6/H3S10ADPr$_4$ nucleosome remodeling data is included for direct comparison. (**D**) Western blot analysis of a FLAG immunoprecipitation (IP) wherein ALC1 is FLAG-tagged and its association with nucleosomes is analyzed in the presence and absence of unmodified or automodified PARP1. The corresponding input (5%) was loaded alongside the IP (elution) lanes for comparison. (**E**) ALC1 remodeling rate constants calculated from data in (**B, C**) and ***Figure 5—figure supplement 2A***. Rate constants were determined by fitting data to a non-linear regression model for one phase exponential decay. Data in (**B**) and (**C**) are represented as mean ± s.d. (n = 3), while the error bars in (**E**) represent 95% CI. Curves in (**B**) and (**C**) represent data fitting to a non-linear regression model for one-phase exponential decay.

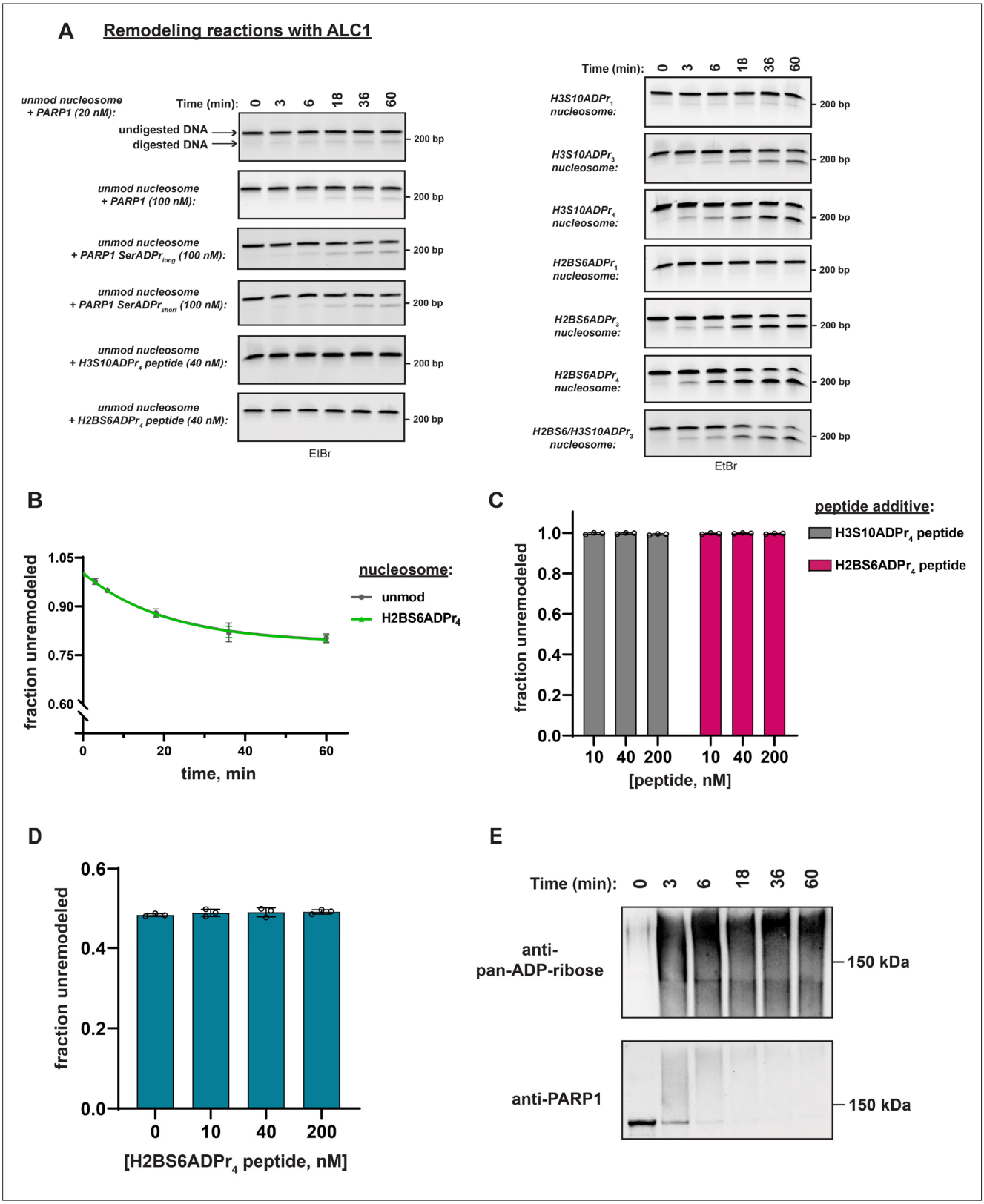

Figure 5—figure supplement 1. Characterization of ALC1 remodeling activity in presence of various macrodomain ligands. (**A**) Representative TBE gel analyses corresponding to recombinant ALC1 time course remodeling activity assay on the indicated nucleosome substrates and peptide additives where applicable. Densitometry values are included in Supplementary Dataset. EtBr = ethidium bromide stain. (**B**) ALC1(1–673) nucleosome remodeling assay time-course for unmodified and H2BS6ADPr$_4$ nucleosome substrates, each at a concentration of 20 nM. The curves represent fit of the data into

Figure 5—figure supplement 1 continued on next page

Figure 5—figure supplement 1 continued

a non-linear regression model for one-phase exponential decay. (**C**) Single time-point (1 h) ALC1 nucleosome remodeling assay wherein each reaction comprises ALC1, an unmodified nucleosome substrate (20 nM), the indicated PARP1 concentration, and NAD^+ (2 mM). Data are represented as mean ± s.d. (n = 3). (**D**) Single time-point (1 h) ALC1 nucleosome remodeling assay wherein each reaction comprises ALC1, $H2BS6ADPr_4$ nucleosome substrate (20 nM), and the indicated concentration of $H2BS6ADPr_4$ peptide. Data are represented as mean ± s.d. (n = 3). (**E**) PARP1 and pan-ADP-ribose western blot analyses following an ALC1 remodeling reaction time-course that includes unmodified nucleosome, PARP1 (20 nM), and NAD^+.

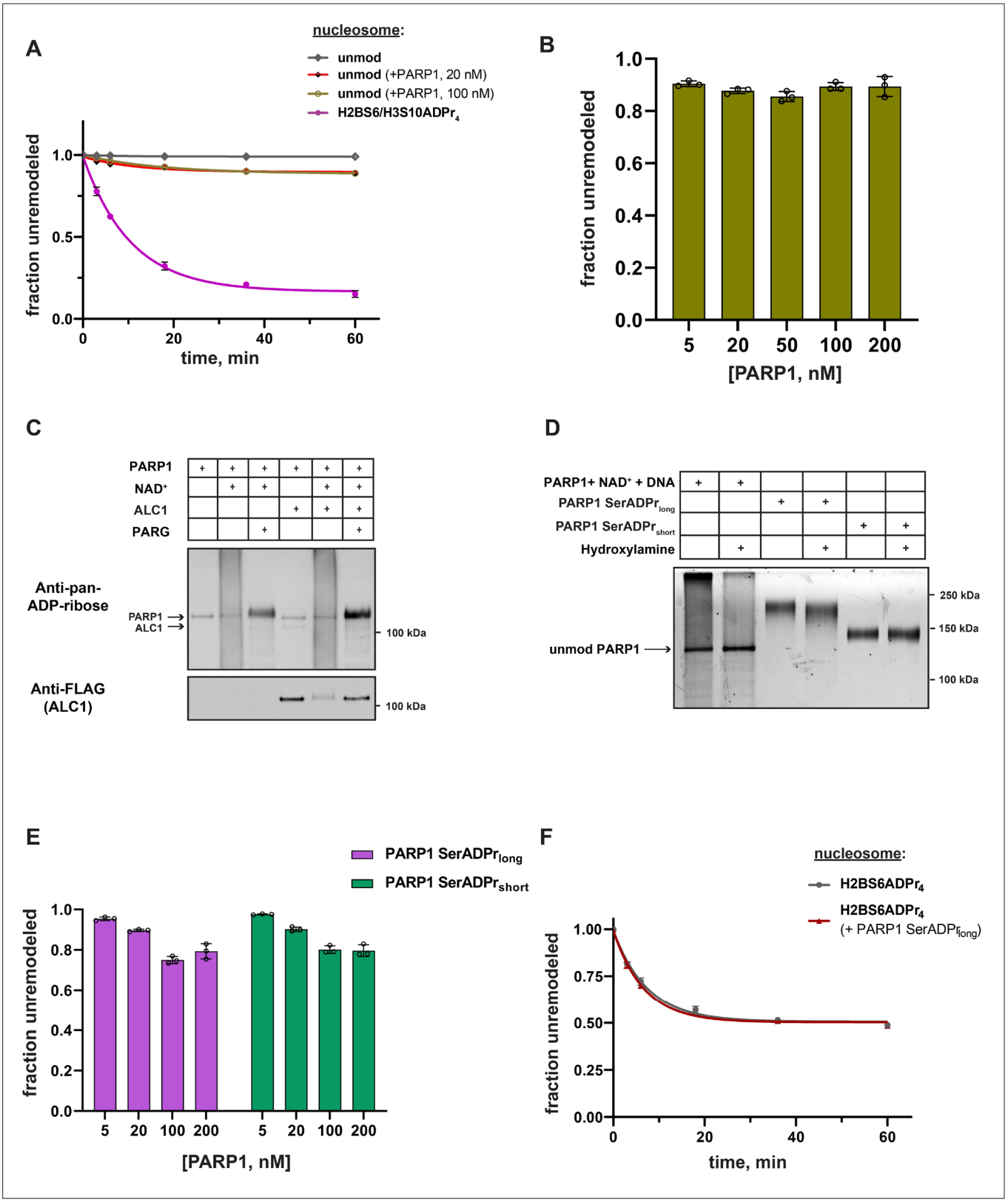

Figure 5—figure supplement 2. Characterization of ALC1 remodeling activity in presence of automodified PARP1. (**A**) ALC1 nucleosome remodeling assay time-course wherein each reaction comprises ALC1 and the indicated nucleosome (20 nM), and the indicated automodified PARP1 concentration. The H2BS6/H3S10ADPr$_4$ nucleosome remodeling data is included for direct comparison. (**B**) Single time-point (1 h) ALC1 nucleosome remodeling assay wherein each reaction comprises ALC1, an unmodified nucleosome substrate (20 nM), and the indicated automodified PARP1 concentration.

Figure 5—figure supplement 2 continued on next page

Figure 5—figure supplement 2 continued

Data are represented as mean ± s.d. (n = 3). (**C**) Pan-ADP-ribose and FLAG western blot analyses of nucleosome remodeling reactions (1 hr) containing the indicated components. PARG was added at a concentration of 1 μM. (**D**) Silver-stained gel image depicting the effect of hydroxylamine treatment on ADP-ribosylated PARP1 modified under different conditions, with and without HPF1. (**E**) Single time-point (1 h) ALC1 nucleosome remodeling assay wherein each reaction comprises ALC1, an unmodified nucleosome substrate (20 nM), and the indicated serine-auto-ADP-ribosylated PARP1 concentration. Data are represented as mean ± s.d. (n = 3). (**F**) ALC1 nucleosome remodeling assay time-course wherein each reaction comprises $H2BS6ADPr_4$ nucleosome substrate at a concentration of 20 nM, with or without PARP1 $SerADPr_{long}$ (100 nM). The curves represent fit of the data into a non-linear regression model for one-phase exponential decay.

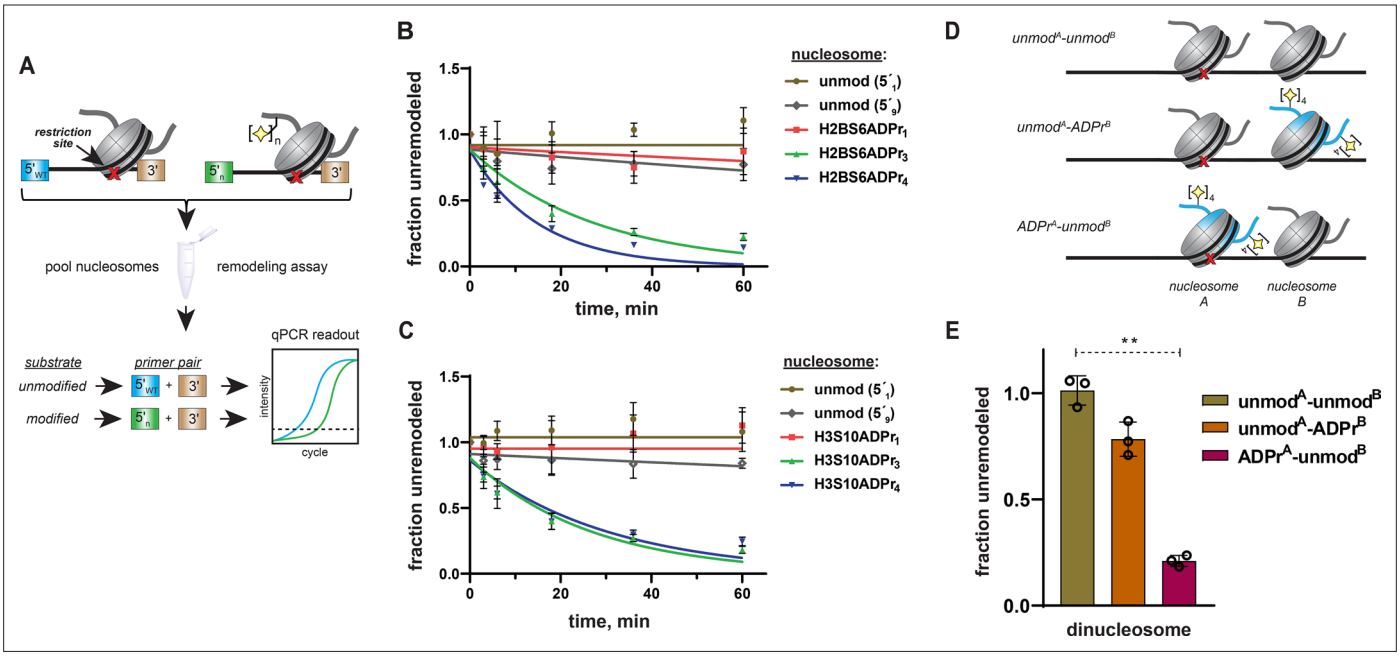

Figure 6. Specificity of ALC1 is preserved in heterogenous nucleosome populations and on asymmetrically ADP-ribosylated dinucleosome substrates. (**A**) Schematic depicting the strategy to prepare heterogenous nucleosome substrate pools and determine ALC1 remodeling activity on specific nucleosomes. (**B**) ALC1 nucleosome remodeling assay time-course for each nucleosome in the histone H2B mixed substrate pool. Two unmodified nucleosomes with different 5′ primer sequences (5′$_1$ and 5′$_9$) were included as internal controls. (**C**) As in (**B**), but with the histone H3 substrate pool. (**D**) A diagram depicting the various dinucleosome constructs assembled in this study. Blue shade represents the modified histone H2B, the red cross represents the PstI restriction site and the yellow star represents the ADP-ribose modification. (**E**), Chromatin remodeling assays with ALC1 on the indicated dinucleosome substrates. ** indicates p-value < 0.001, obtained using an unpaired Student's t-test with Welch's correction. Data in (**B**), (**C**), and (**E**) are represented as mean ± s.d. (n = 3). Curves in (**B**) and (**C**) represent data fitting to a non-linear regression model for one-phase exponential decay.

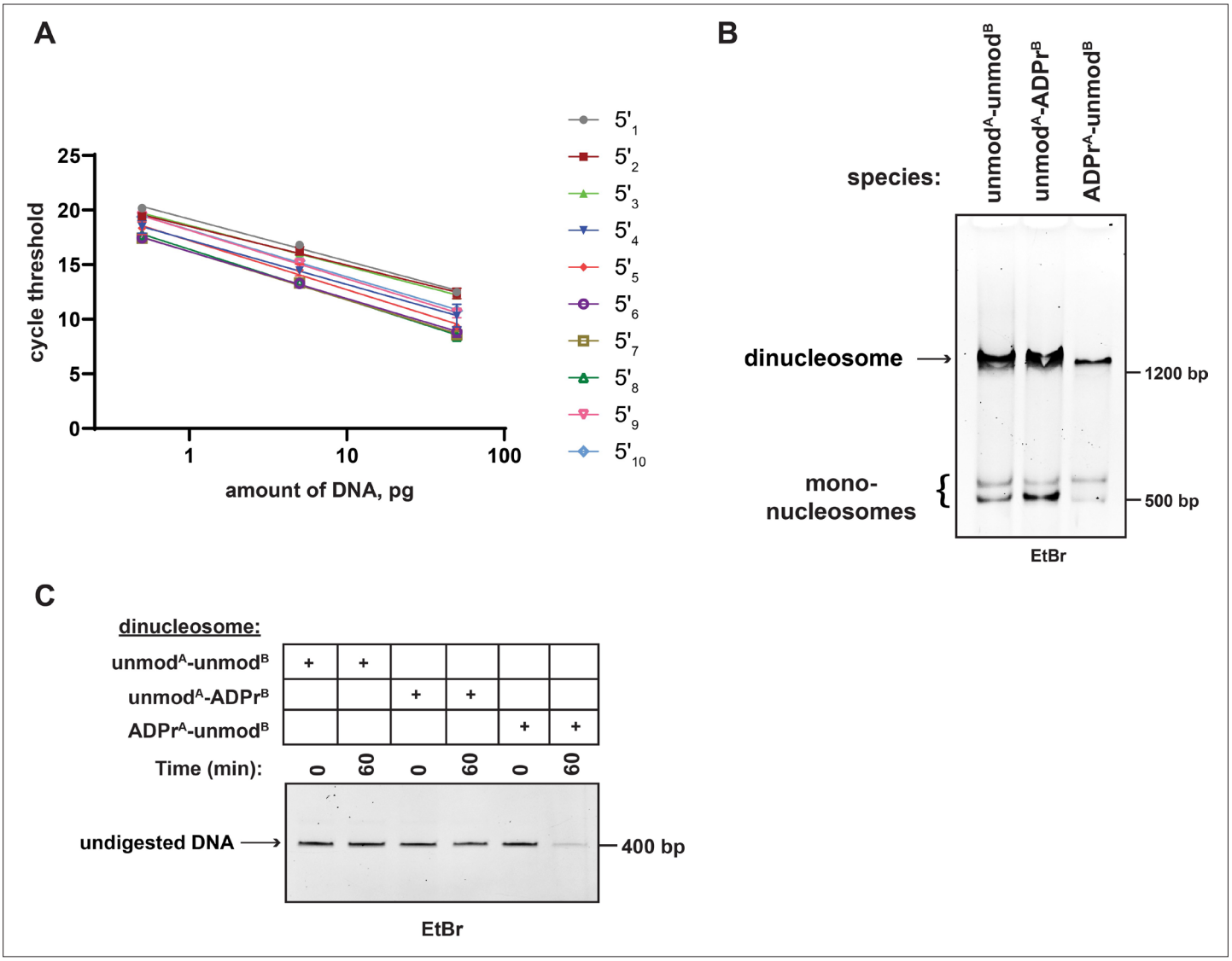

Figure 6—figure supplement 1. ALC1 remodeling analysis on heterogenous nucleosome populations. (**A**) Primer efficiency curves corresponding to all primer:template pairs described in ***Figure 6B and C***. (**B**) Native TBE gel analysis of dinucleosome assembly, which depicts ligation efficiency. EtBr = ethidium bromide stain. (**C**) Representative TBE gel analysis corresponding to ALC1 remodeling activity observed on the indicated dinucleosome substrates. Densitometry values are included in Supplementary Dataset.

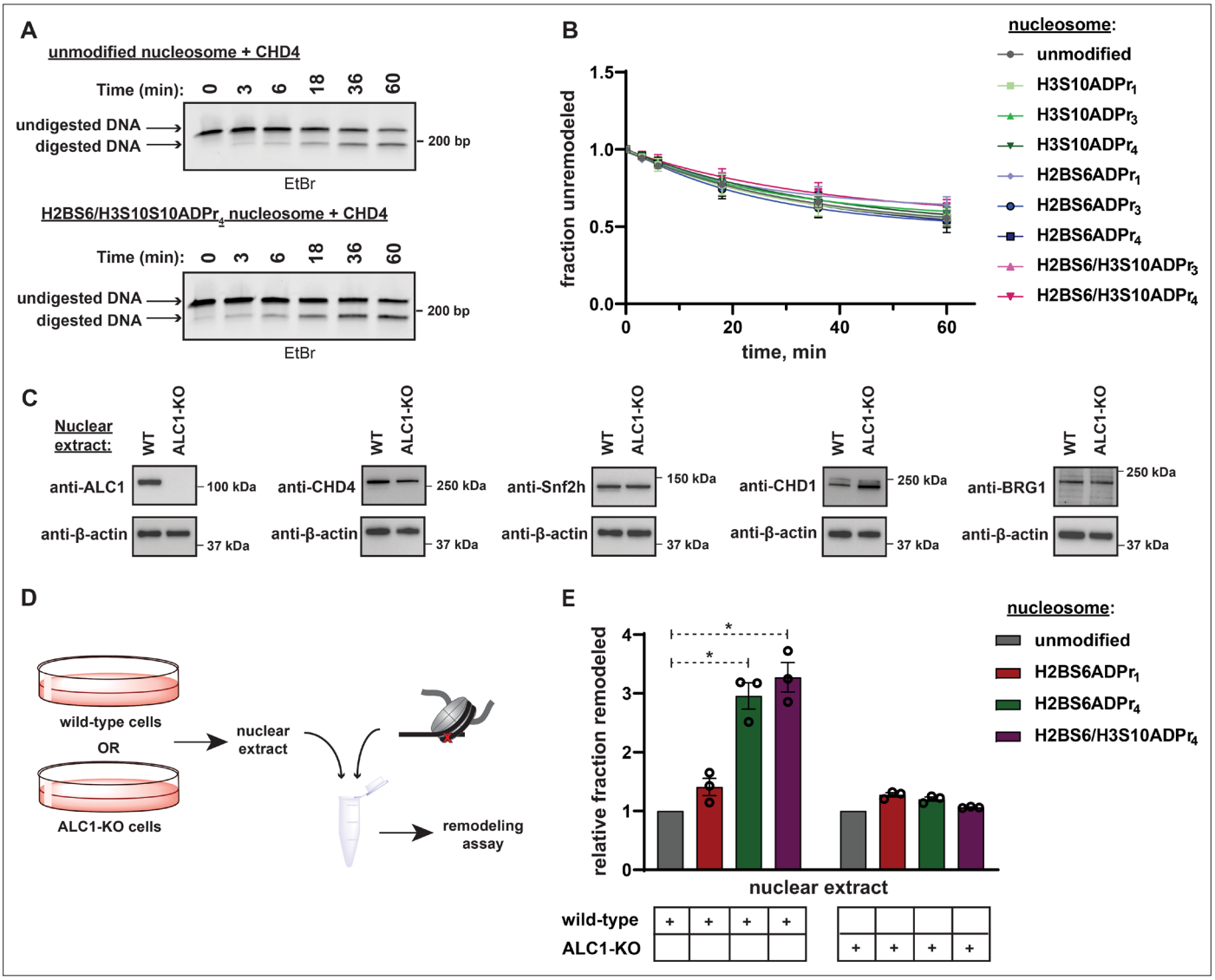

Figure 7. Nucleosome serine ADPr stimulates ALC1-dependent chromatin remodeling activity in nuclear extracts. (**A**) Representative TBE gel analysis from a REA assay corresponding to recombinant CHD4 chromatin remodeling activity on unmodified or H2BS6/H3S10ADPr$_4$ nucleosomes. (**B**) CHD4 nucleosome remodeling assay time-course wherein each reaction comprises CHD4 and the indicated nucleosome substrate. Data are represented as mean ± s.d. (n = 3). Curves represent fit of data into a non-linear regression model for one-phase exponential decay. (**C**) Western blot analysis demonstrating the presence of various chromatin remodelers in the wild-type or ALC1 knock-out (KO) HEK293T nuclear extracts. (**D**) Schematic depicting the strategy to analyze chromatin remodeling activity in wild-type or ALC1-KO HEK293T nuclear extracts. (**E**) Nuclear extract nucleosome remodeling activity assay wherein each reaction comprises the indicated nucleosome substrate and wild-type or ALC1-KO HEK293T cell nuclear extracts. Total remodeling for each ADP-ribosylated nucleosome substrate relative to the unmodified nucleosome substrate in the respective nuclear extract is shown. Data are represented as mean ± s.e.m. (n = 3). * indicates p-value < 0.02, obtained using an unpaired Student's t-test with Welch's correction.

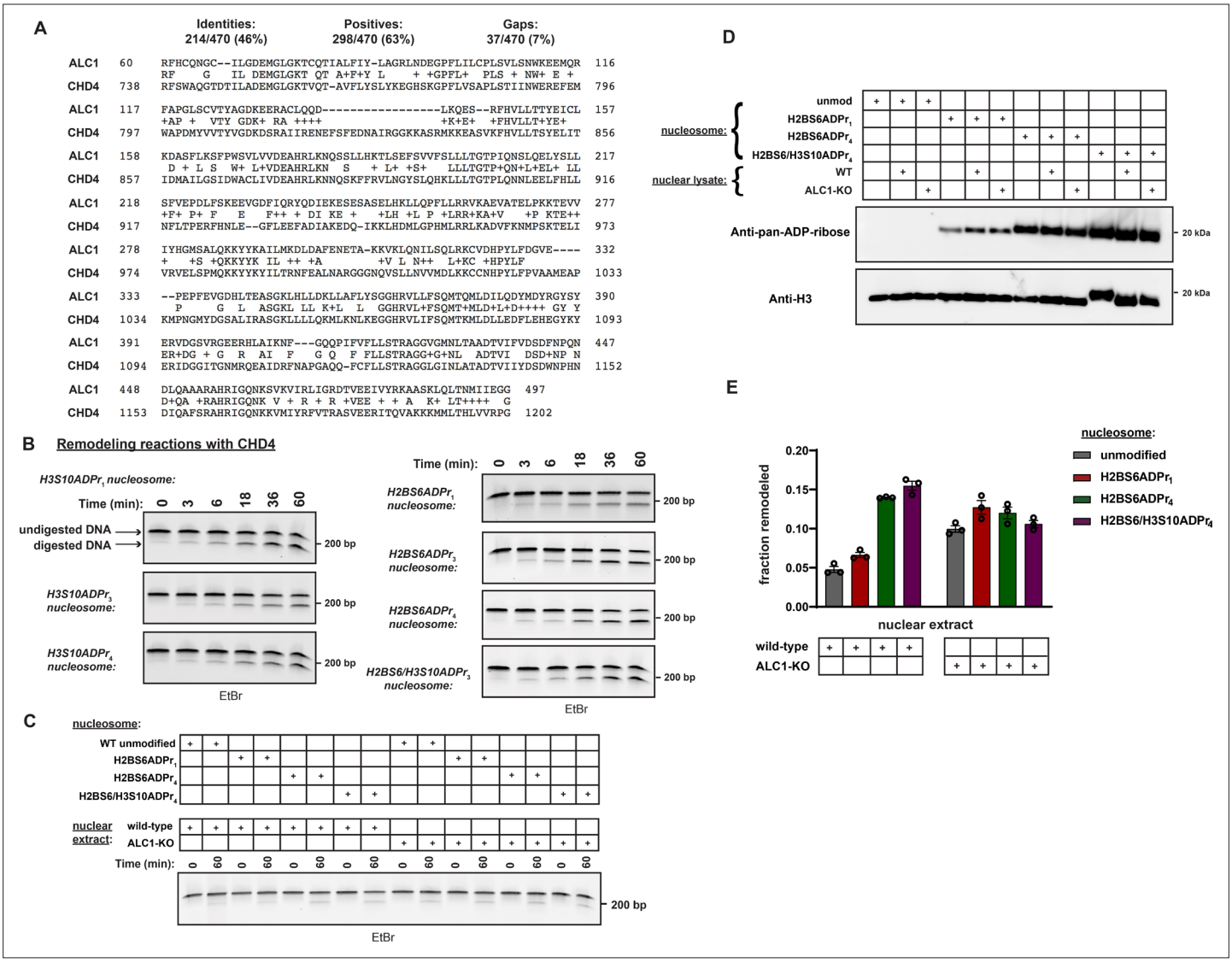

Figure 7—figure supplement 1. H3S10ADPr and H2BS6ADPr specifically sensitize nucleosomes to chromatin remodeling by ALC1. (**A**) BLAST alignment of the ATPase domains from ALC1 (amino acids 60–497) and CHD4 (amino acids 738–1202). (**B**) Representative TBE gel analyses corresponding to recombinant CHD4 time course remodeling activity assay on the indicated nucleosome substrates. Densitometry values are included in Supplementary Dataset. EtBr = ethidium bromide stain. (**C**) Representative TBE gel analyses corresponding to wild-type or ALC1 knock-out (KO) HEK293T nuclear extract chromatin remodeling activity on the indicated nucleosome substrates. Densitometry values are included in Supplementary Dataset. EtBr = ethidium bromide stain. (**D**) Western blot showing the effect of incubating nucleosomes with or without nuclear extract on the ADPr status of the nucleosomes. (**E**) Values for fraction remodeled for each nucleosome substrate in the respective nuclear extract for the experiment in (**C**). Data are represented as mean ± s.e.m. (n = 3).